# A Unified Optimization Method for Real-Time Trajectory Generation of Mobile Robots with Kinodynamic Constraints in Dynamic Environment

Wenhao Luo[1], Jun Peng[2,*], Weirong Liu[2], Jing Wang[3] and Wentao Yu[2]

*Abstract*— **This paper presents an efficient analytic method for a mobile robot to determine a collision-free trajectory with unified optimization. The robot kinodynamic constraints and the geometric constraints due to obstacles are addressed by considering a set of constrained inequalities from parameterized trajectories model. Two optimal performance matrices are employed to assess optimization problems. Particularly, both the constraints and performance functions are incorporated by similar forms in terms of trajectory parameters, which thereby can be considered in a uniform way. A parameter space of adjustable trajectory parameters is constructed to solve the unified optimization problem with constraints and results in more flexible and better optimal performance. The proposed approach is complete and enhances methods of deterministic real-time planning by overcoming typical drawbacks as intermediate configuration, curvature discontinuities, vertical singularities and incomplete optimization. Simulation results verify the validity and superiority of the proposed method.**

## I. INTRODUCTION

The issue of trajectory generation plays a key role in robotic applications and has received lots of efforts [1]. Generally, an effective algorithm should encode problems of feasibility, such as kinematic constraints, kinodynamic constraints and collision avoidance criterion, and optimality to satisfy the need of real-world applications. For on-line planning, the algorithm should also be computationally efficient.

There exist several approaches to consider the mobile robot motion planning with kinematic constraints. To modify holonomic planner to nonholonomic one, the method in [2] makes each consecutive segments of planned path locally satisfy the kinematic constraints. Hierarchical motion planning can be applied to separate the nonholonomic motion planning problem to high-level with discrete space planning and low-level with continuous steering control [3]. Optimal solutions combined with kinodynamic constraints are solved in [4]. However, the compatibility between high-level planner and vehicles dynamic constraints is hard to guaranteed in those hierarchical methodologies.

Another kind of solutions are the search-based methods, including the sampling-based and combinatorial motion planning. The former one may refer to probabilistic roadmap methods(PRM) [5] and rapidly random tree exploring(RRT/RRT*) methods [6][7], which conduct a random sampling search that fast explores the C-space with a sampling scheme governed by collision detection module, and address both vehicle's kinematic and kinodynamic constraints. For the latter methods in [8], they often construct finite roadmaps and find the feasible path by performing discrete graph search in the space. Although these methods perform well in global off-line planning, in local dynamic environment, it may take time to replan the paths on-line due to moving obstacles and the convergence to optimal paths for nonholonomic vehicles may not be ensured for the random search process and the simple graph-based search.

Parametric trajectory generation method pioneered in [9] provides an analytical solution to efficiently handle both robot kinematic constraint and moving obstacles. Later [10] addresses energy-optimal and path length-optimal problems in closed form. However, the resultant trajectory may not be practically feasible due to the kinodynamic constraints. Also, the problem of vertical singularity may appear unless intermediate configuration is added, which could weaken optimal performances. To that end, modified time varying trajectory models are exploited in [11][12], while the optimization is not completely in [11] and robot model in [12] is often difficult to specify. Further research on higher dimensional states as velocity and acceleration (kinodynamic) and complete optimization are needed to better extend application of analytical solutions.

In this paper, the basic idea of the parametric trajectory generation is followed. The objective is to generate trajectories for mobile robots in local unstructured environment with consideration of kinodynamic constraints, collision-avoidance criterion and unified optimization. The trajectory is represented by two polynomials in terms of time so that the velocity and acceleration can be incorporated by derivatives of the polynomial model. The robot kinematic constraint is solved with the differential flatness property. After imposing redefined boundary conditions, kinodynamic constraints and collision avoidance criterion are transferred to several sets of constraint inequalities in terms of adjustable parameters related to the paths. A space of the parameters is constructed, in which the unified optimal solutions considering energy consumption and path length, and those constraints are mapped into corresponding restricted regions or points. Then, the optimized trajectory can be planned by specifying path parameters from the space. Simulation results verify the validity and superiority of the proposed method.

[1]W. Luo is with the Department of Automation, Shanghai Jiao Tong University, and Key Laboratory of System Control And Information Processing, Ministry of Education of China, Shanghai, 200240, China (e-mail:whluo@sjtu.edu.cn).

[2]J. Peng, W. Liu and W. Yu are with the School of Information Science and Engineering, Central South University, and Hunan Engineering Laboratory for Advanced Control and Intelligent Automation, Changsha, 410083, China (e-mail: pengj@csu.edu.cn, frat@csu.edu.cn and wentaoyu@gmail.com).

[*]*Corresponding Author*: J. Peng, pengj@csu.edu.cn

[3]J. Wang is with the Computer Engineering Program, Bethune-Cookman University, Daytona Beach, FL 32114 USA (e-mail: wangj@cookman.edu).

978-1-4799-1201-8/13/$31.00 

This paper is organized as follows. Section II introduces the robot model, trajectory representation and reformulated trajectory generation problems. In section III, kinodynamic constraints and collision avoidance criterion are analytically considered. In section IV, two optimal indexes are developed and suboptimal solutions are given to deal with kinodynamic constraints, collision avoidance and optimization problem on the proposed parameter space. Simulation results are shown in section V. In section VI, conclusions are drawn.

## II. PROBLEM FORMULATION

The mobile robot model with nonholonomic constraints is shown in Fig.1. The guidepoint(GP) is set to be the midpoint of robot's rear wheel-axle. In this paper, the mobile robot can be represented by a simple particle covered by its circumcircle.

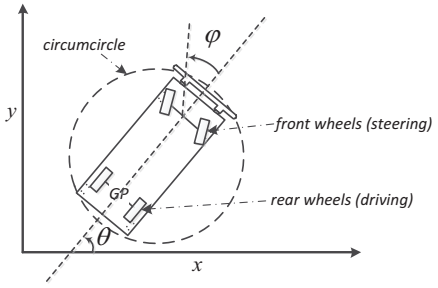


Fig. 1. Mobile robot with nonholonomic constraints

The robot kinematic model can be described as follows.

$$\begin{bmatrix} \dot{x} \\ \dot{y} \\ \dot{\theta} \\ \dot{\varphi} \end{bmatrix} = \begin{bmatrix} cos\theta \\ sin\theta \\ \tan\varphi/l \\ 0 \end{bmatrix} u_1 + \begin{bmatrix} 0 \\ 0 \\ 0 \\ 1 \end{bmatrix} u_2 \tag{1}$$

where $q = [x, y, \theta, \varphi]^T$ is the system state and (x,y) represents the Cartesian coordinates of the middle point of the rear wheel axle. $\theta$ is the orientation of the robot body with respect to the $X$-axis and $\varphi$ is the steering angle. $l$ is the distance between the centers of front wheel-axle and rear wheel-axle. $u_1$ is the driving velocity, and $u_2$ is the steering rate. $\varphi \in (-\pi/2, \pi/2)$ due to the structure constraint of the robot.

Typical parametric trajectory method in [9] is followed, but we specify the robot trajectories by piece-wise parameterized polynomials with respect to time $t$, rather than geometric variables. Then the family of trajectories can be given as follows.

$$\begin{aligned} x(t) &= [c_0 \quad c_1 \quad c_2 \quad \dots \quad c_p]\, f(t) \\ y(t) &= [d_0 \quad d_1 \quad d_2 \quad \dots \quad d_p]\, f(t) \end{aligned} \tag{2}$$

where $f(t) = \begin{bmatrix} 1 & t & t^2 & t^3 & \dots & t^p \end{bmatrix}^T$. $x(t)$ and $y(t)$ are the coordinates of robots guidepoint and integer $p > 0$ is an undetermined order. Considering robots kinematic constraints, the trajectories with the form as (2) should conform at least two conditions. First, at initial time $t_0$ and final time $t_f$ the robot boundary states as $q_0 = [x_0, y_0, \theta_0, \varphi_0]^T$ and $q_f = [x_f, y_f, \theta_f, \varphi_f]^T$ must match the given boundary conditions. Second, the resultant robot steering inputs $u_1$ and $u_2$ should always be defined and maintain continuous.

By imposing the robot model (1) to parametric trajectories (2), we can obtain the reformulated kinematic constraints as

$$\frac{dy}{dx} = \tan\theta, \quad \frac{d^2y}{dx^2} = \frac{\tan\varphi}{l\cos^3\theta} \tag{3}$$

In (3) the kinematic constraints of robots have been reformulated as slope and curvature equations for (2). Based on the differential flatness property, we can further replace them by the velocity and acceleration equations related to differentiates in terms of time $t$. Thus, the typical state vector $q$ could be redefined as $q^* = [x, y, \theta, \varphi, v, a]^T$, where $v$ and $a$ are the driving velocity and the acceleration. Then, it follows from (3) that (initial and final driving velocity and acceleration are $v_0$, $a_0$ and $v_f$, $a_f$ respectively)

$$\begin{cases} \frac{dx}{dt}\big|_{t_0} = v_0\cos\theta_0, & \frac{d^2x}{dt^2}\big|_{t_0} = a_0\cos\theta_0 - \frac{v_0^2\tan\phi_0}{l}\sin\theta_0 \\ \frac{dy}{dt}\big|_{t_0} = v_0\sin\theta_0, & \frac{d^2y}{dt^2}\big|_{t_0} = a_0\sin\theta_0 + \frac{v_0^2\tan\phi_0}{l}\cos\theta_0 \end{cases}$$
$$\begin{cases} \frac{dx}{dt}\Big|_{t_f} = v_f\cos\theta_f, & \frac{d^2x}{dt^2}\Big|_{t_f} = a_f\cos\theta_f - \frac{v_f^2\tan\phi_f}{l}\sin\theta_f \\ \frac{dy}{dt}\Big|_{t_f} = v_f\sin\theta_f, & \frac{d^2y}{dt^2}\Big|_{t_f} = a_f\sin\theta_f + \frac{v_f^2\tan\phi_f}{l}\cos\theta_f \end{cases} \tag{4}$$

In (4) the redefined boundary conditions have been transformed to six independent equations on each axis (including two original equations of $x_0$,$x_f$ or $y_0$,$y_f$). To simplify the discussion, we assume the underdetermined order $p$ in (2) to be six. Then after substituting those conditions, the coefficients vectors of $x(t), y(t)$ would be simplified and determined by only two independent parameters $c_6$ and $d_6$.

To further consider the dynamic environment, we assume the piecewise-constant parameterized trajectory (2) is determined within every time interval $t \in [t_0 + kT_s, t_0 + (k+1)T_s]\,(k = 0, 1, \dots \bar{k}-1)$, coefficients $c_i^k$ and $d_i^k$, $i = 0, \cdots, 6$ are constants, where $T_s$ is the sampling time, and $\bar{k}$ is the maximum integer less than $T/T_s$. Then the boundary equations (4) can be substituted to trajectory in (2), which renders new trajectory model as follows.

$$\begin{aligned} x(t) &= \bar{f}(t)(G^k)^{-1}\left(E^k - H^k c_6^k\right) + c_6^k t^6 \\ y(t) &= \bar{f}(t)(G^k)^{-1}\left(F^k - H^k d_6^k\right) + d_6^k t^6 \end{aligned} \tag{5}$$

where $\bar{f}(t) = \begin{bmatrix} 1 & t & t^2 & t^3 & t^4 & t^5 \end{bmatrix}$, and

$$G^k = \begin{bmatrix} 1 & t_k & t_k^2 & t_k^3 & t_k^4 & t_k^5 \\ 1 & t_f & t_f^2 & t_f^3 & t_f^4 & t_f^5 \\ 0 & 1 & 2t_k & 3t_k^2 & 4t_k^3 & 5t_k^4 \\ 0 & 1 & 2t_f & 3t_f^2 & 4t_f^3 & 5t_f^4 \\ 0 & 0 & 2 & 6t_k & 12t_k^2 & 20t_k^3 \\ 0 & 0 & 2 & 6t_f & 12t_f^2 & 20t_f^3 \end{bmatrix} \tag{6}$$

$$E^k = \begin{bmatrix} x_k & x_f & \frac{dx}{dt}\big|_{t_k} & \frac{dx}{dt}\big|_{t_f} & \frac{d^2x}{dt^2}\Big|_{t_k} & \frac{d^2x}{dt^2}\Big|_{t_f} \end{bmatrix}^T$$

$$F^k = [\ y_k \quad y_f \quad \left.\frac{dy}{dt}\right|_{t_k} \quad \left.\frac{dy}{dt}\right|_{t_f} \quad \left.\frac{d^2y}{dt^2}\right|_{t_k} \quad \left.\frac{d^2y}{dt^2}\right|_{t_f}\ ]^T$$

$$H^k = \left[\ t_k^6 \quad t_f^6 \quad 6t_k^5 \quad 6t_f^5 \quad 30t_k^4 \quad 30t_f^4\ \right]^T$$

It should be noted that since $t_k$ will not be equal to $t_f$, matrix $G^k$ in (7) could avoid singularity problems. Once the specific trajectory expression is obtained, steering control could always be solvable. From (3), considering the slope and curvature of the path, we obtain robot states and steering inputs as follows.

$$\begin{aligned}
\theta &= \arctan\frac{dy}{dx} \\
\cos\theta &= \sqrt{\frac{1}{1+\left(\frac{dy}{dx}\right)^2}} \\
\varphi &= \arctan\left(l\cos^3\theta\cdot\frac{d^2y}{dx^2}\right) \\
u_1 &= \pm\sqrt{\dot{x}^2(t)+\dot{y}^2(t)} \\
u_2 &= lu_1[\frac{(\dddot{y}(t)\dot{x}(t)-\dddot{x}(t)\dot{y}(t))u_1^2}{u_1^6+l^2(\ddot{y}(t)\dot{x}(t)-\ddot{x}(t)\dot{y}(t))^2} \\
&\quad -\frac{3(\ddot{y}(t)\dot{x}(t)-\ddot{x}(t)\dot{y}(t))(\dot{x}(t)\ddot{x}(t)+\dot{y}(t)\ddot{y}(t))}{u_1^6+l^2(\ddot{y}(t)\dot{x}(t)-\ddot{x}(t)\dot{y}(t))^2}]
\end{aligned} \tag{7}$$

According to (5), if boundary conditions are given, the trajectories will only be determined by two parameters as $c_6^k$ and $d_6^k$. In other words, the optimal trajectory generation problem boils down to solve for $c_6^k$ and $d_6^k$ based on constraints due to system model, collision avoidance and optimal performance.

*Remark 2.1:* For $t\in[t_k,t_f)$, the boundary conditions for computing $E^k,F^k$ and $H^k$ are obtained as

$$\begin{aligned}
\tfrac{dx}{dt}\big|_{t_k} &= v_k\cos\theta_k, \quad \tfrac{dy}{dt}\big|_{t_k} = v_k\sin\theta_k \\
\tfrac{d^2x}{dt^2}\big|_{t_k} &= a_k\cos\theta_k - \tfrac{v_k^2\tan\varphi_k}{l}\sin\theta_k \\
\tfrac{d^2y}{dt^2}\big|_{t_k} &= a_k\sin\theta_k + \tfrac{v_0^2\tan\varphi_k}{l}\cos\theta_k
\end{aligned} \tag{8}$$

where $v_k \triangleq u_1(t_k), a_k \triangleq \dot{u}_1(t_k)$, $\theta_k$, and $\varphi_k$ are calculated according to (7) by using the parameterized trajectory $x(t)$ and $(y(t)$ in terms of $c_6^{k-1}$ and $d_6^{k-1}$ at the previous time interval. ◊

## III. FEASIBLE TRAJECTORY GENERATION AMIDST MOVING OBSTACLES

### A. Kinodynamic Constraints

In this paper, kinodynamic constraints are demonstrated by velocity and acceleration bounds. The absolute values of velocity and acceleration bounds on both directions (forward and backward) are assumed to be the same. Consider velocity and acceleration expressions derived from (5), i.e. $\dot{x},\dot{y},\ddot{x}$ and $\ddot{y}$. The kinodynamic constraints are simply as follows.

$$\dot{x}^2(t)+\dot{y}^2(t)\le v_{max}^2, \quad \ddot{x}^2(t)+\ddot{y}^2(t)\le a_{max}^2 \tag{9}$$

where $v_{max}$ and $a_{max}$ are maximum velocity and acceleration respectively. Then substituting those derivatives from (5) into (9), we obtain the following theorem.

**Theorem 1:** For $t\in[t_k,t_f], t_k = t_0+kT_s$, $c_6^k$ and $d_6^k$ must satisfy the following quadratic inequalities to obey kinodynamic constraints.

$$\begin{aligned}
(c_6^k+m_1^k/m_2^k)^2+(d_6^k+m_3^k/m_2^k)^2 &\le v_{\max}^2/(m_2^k)^2 \\
(c_6^k+n_1^k/n_2^k)^2+(d_6^k+n_3^k/n_2^k)^2 &\le a_{\max}^2/(n_2^k)^2
\end{aligned} \tag{10}$$

where

$$\begin{aligned}
&m_1^k=\bar{f}'(G^k)^{-1}E^k, m_2^k=6t^5-\bar{f}'(G^k)^{-1}H^k, m_3^k=\bar{f}'(G^k)^{-1}F^k \\
&n_1^k=\bar{f}''(G^k)^{-1}E^k, n_2^k=30t^4-\bar{f}''(G^k)^{-1}H^k, n_3^k=\bar{f}''(G^k)^{-1}F^k \\
&\bar{f}'=[0\ 1\ 2t\ 3t^2\ 4t^3\ 5t^4], \quad \bar{f}''=[0\ 0\ 2\ 6t\ 12t^2\ 20t^3]
\end{aligned} \tag{11}$$

*Proof:* we assume $v$ and $a$ are current velocity and acceleration of robot, then we have

$$\begin{aligned}
v^2 &= \dot{x}^2+\dot{y}^2 = (m_2^k)^2(c_6^k+\tfrac{m_1^k}{m_2^k})^2+(m_2^k)^2(d_6^k+\tfrac{m_3^k}{m_2^k})^2 \le v_{\max}^2 \\
\therefore &\quad (c_6^k+\tfrac{m_1^k}{m_2^k})^2+(d_6^k+\tfrac{m_3^k}{m_2^k})^2 \le \tfrac{v_{\max}^2}{(m_2^k)^2} \\
a^2 &= \ddot{x}^2+\ddot{y}^2 = (n_2^k)^2(c_6^k+\tfrac{n_1^k}{n_2^k})^2+(n_2^k)^2(d_6^k+\tfrac{n_3^k}{n_2^k})^2 \le a_{\max}^2 \\
\therefore &\quad (c_6^k+\tfrac{n_1^k}{n_2^k})^2+(d_6^k+\tfrac{n_3^k}{n_2^k})^2 \le \tfrac{a_{\max}^2}{(n_2^k)^2}
\end{aligned} \tag{12}$$

$m_2^k$, $n_2^k$ in *Theorem 1* are assumed to be nonzero in most cases. In fact, by numerical analysis, they are close to zero only when $t$ is close to $\frac{t_f-t_0}{2}$ $(m_2^k=0)$, $\frac{t_f-t_0}{4}$ and $\frac{3}{4}(t_f-t_0)$ $(n_2^k=0)$, denoted by $t_v^*$, $t_a^*$ and $t_a^{**}$ respectively. In this case, three additional inequalities should be obeyed as follows.

$$\begin{cases}
(m_1^k)^2_{t=t_v^*}+(m_3^k)^2_{t=t_v^*}\le v_{\max}^2 \\
(n_1^k)^2_{t=t_a^*}+(n_3^k)^2_{t=t_v^*}\le a_{\max}^2 \\
(n_1^k)^2_{t=t_a^{**}}+(n_3^k)^2_{t=t_a^{**}}\le a_{\max}^2
\end{cases} \tag{13}$$

It is noted that these three equations are irrelevant with $c_6^k,d_6^k$, and can be precalculated to decide whether there exists feasible solutions.

### B. Collision Avoidance Criterion

Local dynamic environment is illustrated in Fig.2. The robot velocity and radius are represented by $v_r$ and $r_0$. During one sampling period $t\in[t_0+kT_s,t_0+(k+1)T_s]$ (often small enough), velocity $v_i^k$ of the $i$th obstacle (with radius $r_i$) remains constant. It should be noted that the $i$th static barriers can also be considered covered with circumcircles with radius $r_{si}$ and moving with zero velocity. Motion changing of obstacles can be detected and updated at every sampling instant $t=t_0+kT_s$.

During $t\in[t_0+kT_s,t_f]$ if the $i$th obstacles is considered to be static and relative velocity of the robot to the $i$th obstacle is defined as $(v_{i,x}^k,v_{i,y}^k)$, then the distance between center of the robot and the $i$th obstacle must satisfy:

$$\left(x_i'(t)-x_i^k\right)^2+\left(y_i'(t)-y_i^k\right)^2\ge(r_i+r_0)^2 \tag{14}$$

where $x_i'(t)=x(t)-v_{i,x}^k\tau$, $y_i'(t)=y(t)-v_{i,y}^k\tau$ (relative position of the robot with respect to the static obstacle),

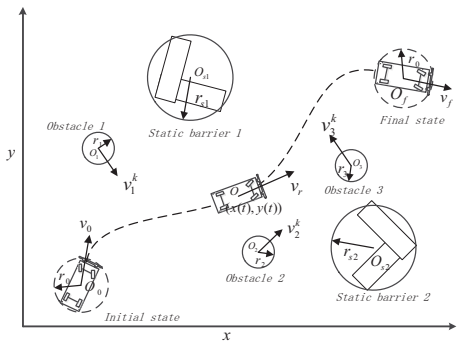


Fig. 2. Mobile robot in the presence of moving obstacles and static barriers.

$\tau = t-(t_0+kT_s)$, for $t \in [t_0+kT_s, t_f]$ (static barriers can also be easily added in).

**Theorem 2:** For $t \in [t_k, t_f], t_k = t_0 + kT_s$, following quadratic inequality with respect to $c_6^k$ and $d_6^k$ must be satisfied to maintain collision free between robot and the $i$th obstacle:

$$(c_6^k + \frac{g_{1,i}^k(t)}{g_{2,i}^k(t)})^2 + (d_6^k + \frac{g_{3,i}^k(t)}{g_{2,i}^k(t)})^2 \geq \frac{(r_i+r_0)^2}{\left(g_{2,i}^k(t)\right)^2} \tag{15}$$

where

$$\begin{aligned} &g_{1,i}^k(t) = \bar{f}(G^k)^{-1}E^k - v_{i,x}^k\tau - x_i^k, \quad g_{2,i}^k(t) = t^6 - \bar{f}(G^k)^{-1}H^k \\ &g_{3,i}^k(t) = \bar{f}(G^k)^{-1}F^k - v_{i,y}^k\tau - y_i^k, \quad \bar{f} = [1 \;\; t \;\; t^2 \;\; t^3 \;\; t^4 \;\; t^5] \end{aligned} \tag{16}$$

*Proof:* Substituting (5) into (14), simplifying and reorganizing it

$$\begin{aligned} &\left(x_i'(t) - x_i^k\right)^2 + \left(y_i'(t) - y_i^k\right)^2 \\ = \;& (g_{2,i}^k(t))^2(c_6^k + \frac{g_{1,i}^k(t)}{g_{2,i}^k(t)})^2 + (g_{2,i}^k(t))^2(d_6^k + \frac{g_{3,i}^k(t)}{g_{2,i}^k(t)})^2 \\ &\geq (r_i+R)^2 \\ \therefore \;& (c_6^k + \frac{g_{1,i}^k(t)}{g_{2,i}^k(t)})^2 + (d_6^k + \frac{g_{3,i}^k(t)}{g_{2,i}^k(t)})^2 \geq \frac{(r_i+r_0)^2}{\left(g_{2,i}^k(t)\right)^2}, \\ &g_{2,i}^k(t) \neq 0 \end{aligned}$$

It is noticed that *Theorem 2* is effective only when $g_{2,i}^k(t) \neq 0$. In fact, numerical analysis on expression of $g_{2,i}^k(t)$ in (16) can prove that $g_{2,i}^k(t) = 0$ only occurs at boundary states, which can be easily pre-identified and considered in application cases.

Since in Section II we have addressed that robot trajectories will only be determined by parameters $c_6^k$ and $d_6^k$, if their corresponding constrained conditions in (15) and (10) are satisfied, a family of kinodynamically feasible and collision free trajectories can be obtained. Finally, specific trajectories with certain value of $c_6^k$ and $d_6^k$ would be eventually selected by unified optimization discussed in next part.

## IV. UNIFIED OPTIMIZATION FOR CANDIDATE FEASIBLE TRAJECTORIES

### A. Energy-Optimal Solution without Moving Obstacles

As in [10], we can use kinematic energy to reflect the energy consumption, then the performance index can be formulated as follows.

$$\min J_k^{E_1}\left(c_6^k, d_6^k\right) = \int_{t_k}^{t_f}(\frac{u_1}{\rho})^2 dt = \frac{1}{\rho^2}\int_{t_k}^{t_f}(\dot{x}^2+\dot{y}^2)dt \tag{17}$$

Both $\dot{x}$ and $\dot{y}$ can be represented in analytical forms with respect to $c_6^k$ and $d_6^k$. Substituting those derivatives into (17), simplifying and reorganizing it, and we could obtain that

$$\begin{aligned} &J_k^{E_1}\left(c_6^k, d_6^k\right) = \frac{1}{\rho^2}\int_{t_k}^{t_f}(\dot{x}^2+\dot{y}^2)dt \\ =&\frac{1}{\rho^2}[s_2(c_6^k + \frac{s_1}{2s_2})^2 + s_2(d_6^k + \frac{s_4}{2s_2})^2 + (s_0+s_3) - \frac{\left(s_1^2+s_4^2\right)}{4s_2}] \end{aligned} \tag{18}$$

where

$$\begin{aligned} &s_0 = \int_{t_k}^{t_f}(\bar{f}'G^{-1}E)^2dt, \quad s_1 = 2\int_{t_k}^{t_f}\left(6t^5 - \bar{f}'G^{-1}H\right)(\bar{f}'G^{-1}E)dt \\ &s_2 = \int_{t_k}^{t_f}\left(6t^5 - \bar{f}'G^{-1}H\right)^2 dt, \quad s_3 = \int_{t_k}^{t_f}(\bar{f}'G^{-1}F)^2dt \\ &s_4 = 2\int_{t_k}^{t_f}\left(6t^5 - \bar{f}'G^{-1}H\right)(\bar{f}'G^{-1}F)dt \end{aligned} \tag{19}$$

From (18) it follows that $J_k^{E_1}\left(c_6^k, d_6^k\right)$ has been reorganized as quadratic form. Thus its minimal value can be achieved as long as

$$c_6^{k*} = -\frac{s_1}{2s_2}, \qquad d_6^{k*} = -\frac{s_4}{2s_2} \tag{20}$$

The point $(c_6^{k*}, d_6^{k*})$ in the plane of $c_6 - d_6$ represents energy-optimal solution of trajectory generation. Since our solution of $(c_6^{k*}, d_6^{k*})$ is analytical and only determined by boundary conditions rather than variable of time $t$, optimal solution has nothing to do with current states of robot. The derivation method implies that optimal method can be updated at each sampling instant $t_k = t_0 + kT_s$ and always aims to reach minimal energy consumption of the rest trajectory.

### B. Length-Optimal Solution without Moving Obstacles

Here a *smallest area* length index is introduced as follows:

$$J_k^{L_1}\left(c_6^k, d_6^k\right) = \int_{t_k}^{t_f}\left[\left(x-x'\right)^2 + \left(y-y'\right)^2\right]dt \tag{21}$$

where

$$x' = \frac{x_f - x_k}{t_f - t_k}(t-t_k) + x_k, \quad y' = \frac{y_f - x_k}{t_f - t_k}(t-t_k) + y_k$$

The formula in (21) is a measure of difference between the planned trajectory and a straight line, on which the coordinates are $(x', y')$ with respect to time. Minimum of (21) implies the smallest area between the planned trajectory and the straight line, which can guarantee the trajectory stays as

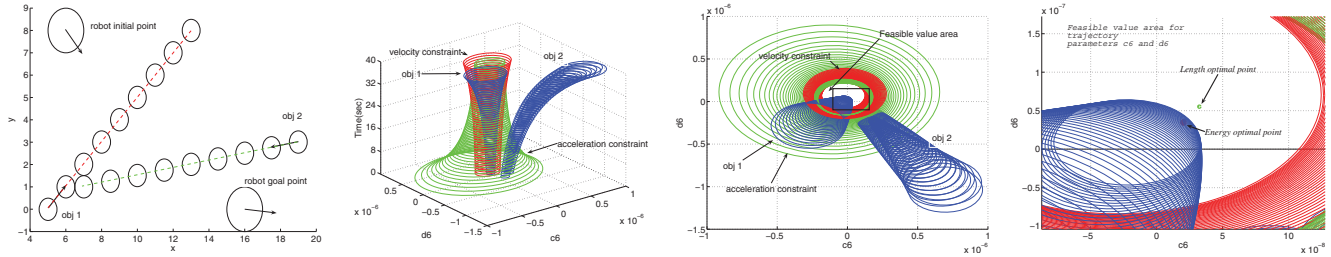


(a) (b) (c) (d)

Fig. 3. The application for parameter space unified-optimization method. (a) the robot initial and final positions in the presence of two moving obstacles 1 and 2. (b) kinodynamic and collision avoidance constraints circles in the parameter space at each moment. (c) constraints circle areas projection on $c_6$-$d_6$ plane. (d) locations of optimal points on $c_6$-$d_6$ plane. This window is amplified from the rectangle area in (c).

close as possible to the initial straight line.

Substituting (5) into (21), simplifying and reorganizing it and we could obtain that

$$\begin{aligned} J_k^{L_1}\left(c_6^k, d_6^k\right) &= \int_{t_k}^{t_f}\left[\left(x-x'\right)^2+\left(y-y'\right)^2\right]dt \\ &= p_2(c_6^k+\frac{p_1}{2p_2})^2+p_2(d_6^k+\frac{p_3}{2p_2})^2+(p_0+p_4) \\ &\quad -\frac{\left(p_1^2+p_3^2\right)}{4p_2} \end{aligned} \tag{22}$$

where

$$\begin{aligned} p_0 &= \int_{t_k}^{t_f}(\bar{f}(G^k)^{-1}E^k-x')^2dt,\ p_2=\int_{t_k}^{t_f}(t^6-\bar{f}(G^k)^{-1}H^k)^2dt \\ p_1 &= 2\int_{t_k}^{t_f}(t^6-\bar{f}(G^k)^{-1}H^k)(\bar{f}(G^k)^{-1}E^k-x')dt \\ p_3 &= 2\int_{t_k}^{t_f}(t^6-\bar{f}(G^k)^{-1}H^k)(\bar{f}(G^k)^{-1}F^k-y')dt \\ p_4 &= \int_{t_k}^{t_f}(\bar{f}(G^k)^{-1}F^k-y')^2dt \end{aligned} \tag{23}$$

Similarly, $J_k^{L_1}\left(c_6^k, d_6^k\right)$ in (21) has been reorganized as quadratic form. Thus, its minimal value can be achieved as long as

$$c_6^{k**}=-\frac{p_1}{2p_2},\qquad d_6^{k**}=-\frac{p_3}{2p_2} \tag{24}$$

Substituting $p_1$, $p_2$ and $p_3$ into (24), we can achieve the analytical solution of $c_6^{k**}$ and $d_6^{k**}$, which could then render a length-optimal trajectory. Similar to the energy-optimal solution, such an analytical solution is also obtained in closed form and can be updated at each sampling instant, which is good for real-time planning.

### *C. Integration of Constraints and Optimal Solutions on Parameter Space*

In the previous discussions, both constraints and performance expressions are formulated by analytic quadratic forms in (10), (15), (18) and (22) with respect to variables $c_6^k$ and $d_6^k$. To that end, we can reformulated them on the plane of those two parameters (*the parameter space*), and rely on their respective significance on the plane to find out the expected solutions of $(c_6^k, d_6^k)$.

Considering kinodynamic and collision avoidance inequalities (10) and (15), both of them can be represented by sets of circle areas in the parameter space. For $t\in\left[t_k,t_f\right], t_k = t_0+kT_s$, the feasible value area for $c_6^k$ and $d_6^k$ under (10) is the interior region of both velocity and acceleration circles $\Theta_{v,t}^k$ and $\Theta_{a,t}^k$. For collision avoidance, each moving obstacle has a corresponding feasible area for $c_6^k, d_6^k$ according to (15), which is exterior region of the collision circles $\Theta_{c,t}^k$. The respective feasible areas of those constraints for the two parameters and the integrated one are as follows.

$$\begin{aligned} \Theta_{c,t}^k &= \{(c_6^k,d_6^k)|(c_6^k+\frac{g_{1,i}^k}{g_{2,i}^k})^2+(d_6^k+\frac{g_{3,i}^k}{g_{2,i}^k})^2 \\ &\quad \geq \frac{(r_i+R)^2}{(g_{2,i}^k)^2}, i=1,2...\} \\ \Theta_{v,t}^k &= \{(c_6^k,d_6^k)|(c_6^k+\frac{m_1^k}{m_2^k})^2+(d_6^k+\frac{m_3^k}{m_2^k})^2\leq\frac{v_{\max}^2}{(m_2^k)^2}\} \\ \Theta_{a,t}^k &= \{(c_6^k,d_6^k)|(c_6^k+\frac{s_1^k}{s_2^k})^2+(d_6^k+\frac{s_3^k}{s_2^k})^2\leq\frac{a_{\max}^2}{(s_2^k)^2}\} \end{aligned} \tag{25}$$

$$\Theta_f^k=\bigcap_{t\in[t_k,t_f]}(\Theta_{c,t}^k\cap\Theta_{v,t}^k\cap\Theta_{a,t}^k), k=1,2...\bar{k} \tag{26}$$

To satisfy all the constrained conditions, the candidate parameter point $(c_6^k, d_6^k)$ should be located at the intersection of those constrained areas (25) on the parameter space, i.e. $(c_6^k, d_6^k)$ belongs to the interior region denoted by $\Theta_f^k$.

For optimal solutions in (20) and (24), optimal performance can be achieved by directly selecting centers of two circles forms as (18) and (22) in the parameter space, i.e. $O_e(-\frac{s_1}{2s_2},-\frac{s_4}{2s_2})$ and $O_l(-\frac{p_1}{2p_2},-\frac{p_3}{2p_2})$. These optimal points remain fixed in parameter space until next updating time. If constraints are incorporated, then the suboptimal points of $(c_6^k, d_6^k)$ are needed. An example is given in Fig.3.

In Fig.3(a), the mobile robot should move from initial point to goal point and maintain collision free with two moving obstacles. The entire operation time is set to be 40s and obstacles motion remain constant. Constraints areas in terms of $c_6^k$ and $d_6^k$ at each moment are plotted in Fig.3(b). Kinodynamic constraints circles are red ones and green ones respectively(velocity and acceleration). Collision avoidance constraints areas are blue ones of those two obstacles. Since obstacles' motion is fixed in this case, $c_6^k$ and $d_6^k$ will not be

updated and remain constant as $c_6$ and $d_6$. Then for the entire maneuver time, specified points $(c_6, d_6, t)$ should be inside the red and green columnar areas, while maintain outside the two blue columnar areas of two obstacles. Such feasible value area can be found by projection on $c_6$-$d_6$ plane and represented by the blank area marked in Fig.3(c), which is in fact the area of $\Theta_f^k$ formulated in (26).

Energy-optimal and length-optimal points $O_e$(red) and $O_l$(green) are plotted in Fig.3(d). The energy optimal point is inside the projection of collision constraints area. In such case, suboptimal solutions are needed. Expressions of two optimal performance indexes as (18) and (22) indicate that, the closer is the candidate point $O(c_6^k, d_6^k)$ to $O_e$ or $O_l$, the better the corresponding optimal performance will be. To this end, suboptimal points can be selected if only they are closer to optimal points while satisfying location requirements of those constraints areas. *For unified optimization purpose*, we can switch the optimal mode smoothly by choosing various candidate points $O$ between $O_e$ and $O_l$, and continuously alter the different 'weight' of line segments $OO_e$ and $OO_l$ to meet various optimal requirements (energy oriented, length oriented or balanced optimality).

*Remark 4.1:* The proposed method is complete. The solvable condition for $(c_6^k, d_6^k)$ depends on the existence of $\Theta_f^k$. In fact, if kinodynamic circles don't intersect, or the intersection is totally inside the collision circles, it indicates that under current kinodynamic constraints and given manuever time, the motion planning problem does not have a solution. An alternative way is to extend $t_f$ until the feasible value field $\Theta_f^k$ becomes nonempty. ◊

*Remark 4.2:* When the number of obstacles increases, it is not necessary to study the whole parameter space to find the suboptimal solution even if the optimal solution lies in collision circles due to those obstacles. Only solutions within the intersection region of kinodynamic circles are considered, which is a relatively small and limited set, since kinodynamic feasibility must be guaranteed ahead. Also, the algorithm merely considers detected obstacles at present sampling interval, so the space will not always be filled up with collision circles as the complete map may appear to. ◊

## V. SIMULATION

This section describes the simulation results to verify the effectiveness of our approach. First, we consider the situation that robot moves in an unstructured environment without other constraints. Our approach is compared against the typical geometric analytical solution and its optimal extension proposed in [9] and [10], and the time-variants model based analytical solution in [11]. All quantities conform to a given unit system. The settings are as follows:

- Robot settings: $r_0$=1, $l$=0.8.
- Boundary Conditions: $q_0^* = \left(0, 0, -\frac{\pi}{4}, 0, 0.4, 0\right)$ and $q_f^* = \left(17, 10, -\frac{\pi}{4}, 0, 0.2, 0\right)$.
- Maneuver time: $t_0$=0, $t_f$=40s.

In Fig.4 there are five trajectories generated by different methods. Among them, path 1 is computed by our energy-optimal approach. Path 2 is generated by time-variant parametric model based approach [11]. Path 3 and 4 are based on near minimum energy and near shortest path solutions in [10] respectively. Path 5 is generated by typical geometric analytic solution in [9]. It is straightforward that path 1 has less swings and detours than other four pathes. Detailed data about energy consumption and path length are also provided in Fig. 5(a) and Fig. 5(b) respectively. From these figures, it is noticed that our optimal approach in principle outweigh these typical solutions in both energy consumption and path length. In fact, after fitting different trajectory model, the uniform parameter space can also be exploited to assess these analytic solutions as well. For instance, considering method in [11], its suboptimal solution is merely specified by approaching length optimal points horizontally or vertically, while our method can directly specify those parameters by optimal solution.

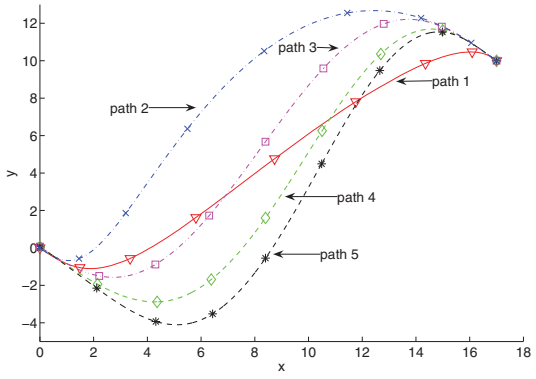


Fig. 4. The trajectories comparison of mobile robot without obstacles and constraints.

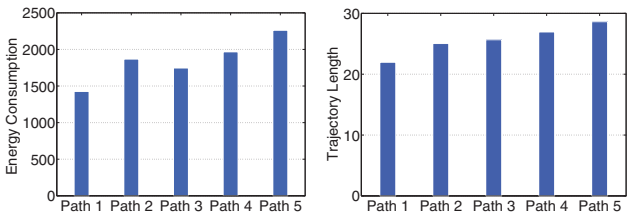


Fig. 5. Performance of energy consumption and path length of those trajectories in Fig.4. (a) Energy consumption (b) Trajectory length.

To consider our optimal approach towards trajectory generation problem under dynamic environment, several static and dynamic obstacles are added to create a cluttered environment. Updated settings of such a scenario are as follows.

- Robot kinodynamic constraints: $v_{max}$=0.9, $a_{max}$=0.1. Initial coordinates of the *three moving obstacles*: $O_1(t_0) = [5.3, -0.7]^T, O_2(t_0) = [13.5, 7.6]^T, O_3(t_0) = [15.9, 14.4]^T$.
- Radius of dynamic and static obstacles: $r_i$=0.5($i$=1,...,10).
- Redefined robot boundary conditions: $q_0^* = \left(-5, 6, -\frac{\pi}{4}, 0, 0.6, 0\right)$ and $q_f^* = \left(23, 10, -\frac{\pi}{4}, 0, 0.4, 0\right)$.
- Starting time and ending time: $t_0$=0, $t_f$=40s.
- Velocities of the three moving obstacles from t=0s and

change from t=20s :
$v_1^0 = (-0.1, 0.4)^T$, $v_1^1 = (0.15, 0.35)^T$
$v_2^0 = (-0.5, -0.1)^T$, $v_2^1 = (-0.5, -0.05)^T$
$v_3^0 = (-0.15, -0.15)^T$, $v_3^1 = (0.15, -0.1)^T$
Sampling period is chosen to be Ts=10s.

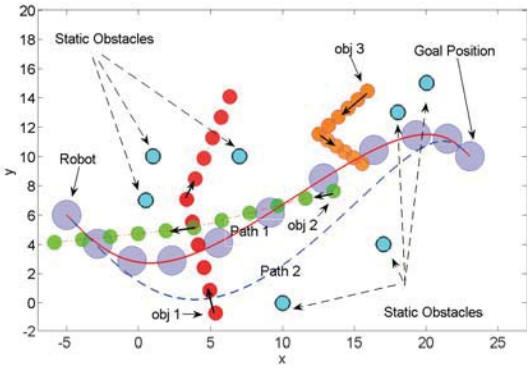


Fig. 6. Trajectory generation in cluttered environment. Path 1 is generated by our length optimal approach. Path 2 is computed by length optimal method in [11].

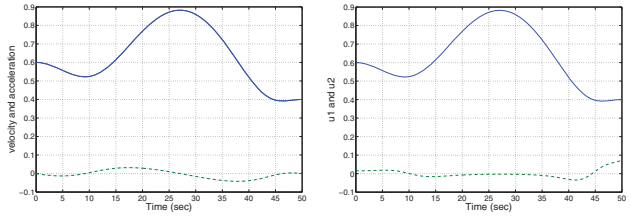


(a) (b)

Fig. 7. Trajectory of robot motion. (a)Trajectories of robot velocity and acceleration. (b)Trajectories of robot inputs u1 and u2.

In Fig.6, robot is expected to move through the cluttered environment containing three moving obstacles and seven static ones. The optimal objective is to find a shortest collision free path. The robot and three moving obstacles are printed every 4 seconds. It is noticed that the red path 1 by our length-optimal approach is collision-free during the entire operation. The blue path 2 generated by [11] is also free from collision, while it has a longer swing, which makes it more conservative. The typical geometrical methods as [10] may not be able to handle such a cluttered environment, since in those methods robot velocity on one axis is always fixed, thus making it vulnerable to potential collisions. The corresponding motion trajectory of path 1 is provided in Fig.7. The inputs are smooth and both velocity and acceleration well satisfy the given kinodynamic bounds. If the environment becomes more cluttered, the feasible value field for $(c_6^k, d_6^k)$ may not exist. In that case, we shall extend the maneuver time $t_f$ until feasible solution can be found, such that robot has more time to run a bigger detour to avoid those obstacles. Since the two optimal solutions are uniformly defined in the parameter space, integrated metric that embeds both indexes and their respective weights can be applied to achieve unified optimization. Other shapes of obstacles may also be handled by their closed algebraic description, and the collision avoidance criterion (14) still works if obstacle center coordinates and radius can be replaced by dangerous point and safety margin of the obstacles, and if the resultant constraints inequalities are also 1st- or 2nd-order.

## VI. CONCLUSIONS

This paper presents an approach to solve unified trajectory optimization problem for mobile robot moving in local unstructured environment. Higher dimensional states such as velocity and acceleration are incorporated to enable more flexible motion control. Kinodynamic constraints and collision avoidance criterion are transferred to constrained inequalities in terms of adjustable trajectory parameters, which can be embedded in the proposed parameter space together with two performance indexes. The unified-optimization thereby becomes a simple geometrical problem and is solved in closed form for real-time planning. Simulation results have verified the effectiveness and superiority of the proposed method. Such a method could also be exploited for local trajectory optimization in search-based methods.

## VII. ACKNOWLEDGMENT

The authors would like to acknowledge that this work is partially supported by National Natural Science Foundation of China No. 61071096, 61073103, 61003233, and Specialized Research Found for Doctoral Program of Higher Education No. 20100162110012 and No. 20110162110042.

## REFERENCES

[1] S. M. LaValle, *Planning algorithms*. Cambridge University Press, 2006.
[2] J.-P. Laumond, P. E. Jacobs, M. Taix, and R. M. Murray, "A motion planner for nonholonomic mobile robots," *IEEE Transactions on Robotics and Automation*, vol. 10, no. 5, pp. 577–593, 1994.
[3] A. Rosiglioni and M. Simina, "Kinodynamic motion planning," in *IEEE International Conference on Systems, Man and Cybernetics*, vol. 3, 2003, pp. 2243–2248.
[4] X.-C. Lai, S. S. Ge, and A. Al Mamun, "Hierarchical incremental path planning and situation-dependent optimized dynamic motion planning considering accelerations," *IEEE Transactions on Systems, Man, and Cybernetics, Part B: Cybernetics*, vol. 37, no. 6, pp. 1541–1554, 2007.
[5] J. Van Den Berg and M. Overmars, "Kinodynamic motion planning on roadmaps in dynamic environments," in *IEEE/RSJ International Conference on Intelligent Robots and Systems*, 2007, pp. 4253–4258.
[6] S. M. LaValle and J. J. Kuffner, "Randomized kinodynamic planning," *The International Journal of Robotics Research*, vol. 20, no. 5, pp. 378–400, 2001.
[7] S. Karaman and E. Frazzoli, "Sampling-based algorithms for optimal motion planning," *The International Journal of Robotics Research*, vol. 30, no. 7, pp. 846–894, 2011.
[8] J. E. Goodman and J. O'Rourke, *Handbook of discrete and computational geometry*. CRC press, 2010.
[9] Z. Qu, J. Wang, and C. E. Plaisted, "A new analytical solution to mobile robot trajectory generation in the presence of moving obstacles," *IEEE Transactions on Robotics*, vol. 20, no. 6, pp. 978–993, 2004.
[10] J. Yang, Z. Qu, J. Wang, and K. Conrad, "Comparison of optimal solutions to real-time path planning for a mobile vehicle," *IEEE Transactions on Systems, Man and Cybernetics, Part A: Systems and Humans*, vol. 40, no. 4, pp. 721–731, 2010.
[11] Y. Guo and T. Tang, "Optimal trajectory generation for nonholonomic robots in dynamic environments," in *IEEE International Conference on Robotics and Automation*, 2008, pp. 2552–2557.
[12] H. Yuan and T. Shim, "Model based real-time collision-free motion planning for nonholonomic mobile robots in unknown dynamic environments," *International Journal of Precision Engineering and Manufacturing*, vol. 14, no. 3, pp. 359–365, 2013.